PHYSICAL REVIEW B VOLUME 52, NUMBER 1 1 JULY 1995-I

Anharmonicity effects on the extendend x-ray-absorption fine structure: The case of β-AgI

G. Dalba, P. Fornasini, and R. Gotter
Dipartimento di Fisica, Università degli Studi di Trento, I-38050 Povo (Trento), Italy

F. Rocca
Centro di Fisica degli Stati Aggregati ed Impianto Ionico, Consiglio Nazionale delle Ricerche e Istituto Trentino di Cultura, I-38050 Povo (Trento), Italy

(Received 26 January 1994; revised manuscript received 13 January 1995)

Anharmonicity effects on the extended x-ray-absorption fine structure (EXAFS) of β-AgI have been studied within the temperature range 77–410 K through the cumulant analysis of the first-shell contribution. The distributions of I-Ag distances and the corresponding pair potentials have been reconstructed directly from cumulants. The shape of the EXAFS pair potential is temperature independent, while its equilibrium position shifts to lower values with increasing temperature. The I-Ag thermal expansion is influenced not only by the EXAFS pair-potential anharmonicity but also by its shift, so that ΔC_1 is not equal to the ratio $C_3/2C_2$. Thermal expansion measured by EXAFS is significantly larger than the one measured by diffraction; the difference is due to vibrational motion normal to the I-Ag bond direction, responsible also for peculiar correlation effects on the mean square relative displacement (MSRD). The distribution of I-Ag distances sampled by EXAFS is consistent not only with the excluded-volume model but also with vibrational models leading to strong distortions of the first-shell tetrahedral cage. Harmonic and anharmonic contributions to the I-Ag MSRD have been singled out, the anharmonic fraction amounting to 20% at 300 K.

I. INTRODUCTION

Thermal and static disorder affect the amplitude and phase of the extended x-ray-absorption fine structure (EXAFS). The standard formula for EXAFS analysis, within the one-electron single-scattering harmonic approximation, accounts for disorder by one amplitude-damping parameter for each coordination shell, the EXAFS Debye-Waller factor $\exp(-2k^2\sigma_j^2)$.[1] When the harmonic approximation breaks down, the standard EXAFS formula can lead to errors in the determination of the structural and thermal parameters.[2,3] This happens when studying systems with relatively low Debye temperatures or with large static disorder. Also in systems with relatively high Debye temperatures, however, while the first-shell signal can be analyzed within the harmonic approximation, the outer-shell signals can be affected by anharmonicity.[4]

The treatment of anharmonicity in EXAFS can be done by the cumulant method.[5,6] Basically, the EXAFS signal is expanded as a series of cumulants of the distribution of interatomic distances. Even and odd cumulants determine the amplitude and phase of EXAFS, respectively. The second cumulant is the variance σ^2 of the distribution, the mean-square relative displacement (MSRD) considered also in harmonic approximation.[7] Higher-order cumulants characterize the shape of the distribution: They are zero for Gaussian distributions. The cumulant analysis of EXAFS can be utilized to check the relevance of anharmonicity and the applicability of the standard formula.[8] More appealing is the possibility of obtaining quantitative information on the structural and thermal properties of anharmonic systems. If the cumulant series is fastly convergent, the leading cumulants (typically the first four) can be determined from EXAFS with reasonable accuracy. Their knowledge allows one to reconstruct the low-k missing part of the signal and the distance distribution.[9,10]

The standard EXAFS formula contains three parameters for each coordination shell (interatomic distance, coordination number, and Debye-Waller factor) whose structural interpretation is immediate. Assigning a direct structural meaning also to EXAFS cumulants of anharmonic systems is by far less immediate.

EXAFS analysis gives the cumulants C_i of an *effective* distribution of distances,[5] which differ from the cumulants of the *real* distribution. This difference, growing with disorder, is generally taken into account for the first cumulant, but has not yet been quantified for higher-order cumulants.

The temperature dependence of the first cumulant C_1 gives information on the thermal expansion of solids. To this purpose the ratio $C_3/2C_2$ is sometimes considered equivalent to (and even more accurate than) ΔC_1;[11,12] this assumption should, however, be checked against the difference between the crystal potential and pair potential sampled by EXAFS.[13] Moreover, C_1 is an average of interatomic distances, and is in principle different from the crystallographic distance between average interatomic positions.[14] The determination of thermal expansion from EXAFS could then be biased by large vibrational motions.

Cumulants can be expressed as a power series of temperature, with the coefficients depending on the force

constants of the EXAFS pair potential.[15] To leading order, C_2 is linear in T (high-temperature harmonic approximation), C_3 is quadratic, and C_4 is cubic. A T^2 and T^3 behavior is generally assumed for C_3 and C_4 in the literature.[16] The negligibility of higher-order terms depends on the nature of the actual interatomic potential.

In particular, the anharmonic deviation of the second cumulant C_2 from Einstein-like behavior (linear at high temperatures) (Ref. 6) cannot easily be determined by direct inspection of the plot of C_2 versus temperature.[10] Its evaluation and subtraction is, however, necessary to achieve accurate comparisons of the EXAFS MSRD with harmonic calculations. The difference between the EXAFS MSRD and the uncorrelated atomic mean-square displacements (MSD) obtainable from diffraction[14] is the displacement correlation function (DCF):[7] The ability to reproduce the DCF is a test for phonon eigenvectors obtained from vibrational dynamics models or *ab initio* calculations.[17]

The aim of the present paper is to show how an accurate cumulant analysis of EXAFS spectra allows, if proper convergence properties are met, the characterization of the local structure and dynamics of anharmonic systems, not only through reconstruction of the distance distributions, but also separately studying the temperature dependence of each cumulant. To this purpose β-AgI is particularly well suited: It exhibits anharmonicity already at relatively low temperatures[18] and its thermal expansion coefficient has a rather peculiar behavior;[19] besides, a thorough EXAFS study has already been done based on the optimization of a realistic excluded-volume structural model.[20] The effectiveness of the cumulant method for studying the distance distributions in β-AgI was demonstrated in a previous paper.[10]

We present here EXAFS measurements at the L_3 edge of iodine in β-AgI from 77 to 410 K and the analysis of the first-shell signal (distance I-Ag) by the cumulant method. We have reconstructed from experimental cumulants the distributions of distances and (in the classical limit) the EXAFS pair potentials. The temperature dependence of cumulants has then been correlated to the pair potential. The procedure is exclusively based on experimental data (including the estimate of the convergence of cumulant series); it has allowed us to single out the anharmonic contributions to the MSRD, to study the relationship between the the thermal expansion and anharmonicity of the EXAFS pair potential, and to evidence the difference between thermal expansion measured by EXAFS and by diffraction. The comparison with the analysis of Ag K EXAFS (Ref. 10) has permitted us to quantitatively assess the uncertainty of the cumulant method and to critically reconsider some previous results.

By separately considering the temperature dependence of cumulants and its relationship with vibrational dynamics, new insights have been gained on the structural interpretation of EXAFS data for AgI with respect to the excluded-volume model.

This paper is organized as follows. Section II contains a synthetic account of EXAFS measurements and data analysis. In Sec. III the procedure utilized to reconstruct the distance distributions, the EXAFS pair potentials, and the temperature dependence of cumulants is described and critically analyzed. Section IV is dedicated to conclusions.

II. EXAFS MEASUREMENTS AND DATA ANALYSIS

For the purpose of the present work we made a new set of measurements at the L_3 edge of iodine in the temperature range 77–410 K. The procedure of sample preparation has been described elsewhere.[21,22] EXAFS measurements were done at the PWA-BX1 beam line of the Frascati Laboratories. The electron energy, maximum current, and wiggler magnetic field were 1.5 GeV, 60 mA, and 1.6 T, respectively. The monochromator was a silicon channel-cut crystal with (111) reflecting faces. The signal was monitored by argon-filled ionization chambers. The overall energy resolution was estimated to be about 0.8 eV. The sample was mounted on the cold finger of a liquid-nitrogen cryostat; the temperature was controlled up to 410 K by a thermoresistance with an estimated accuracy of $\pm$ 2 K.

A relative calibration of the energy scales of all spectra was achieved to within 0.1 eV. The values of the photoelectron wave vector k were calculated with respect to an energy origin E_0 set at the maximum of the first derivative of each spectrum. The EXAFS function was determined as $\chi(k) = [\mu(k) - \mu_1(k)]/\mu_0(k)$, where $\mu(k)$ is the experimental absorption coefficient, $\mu_1(k)$ a spline polynomial best fitting the average behavior of $\mu(k)$, and $\mu_0(k)$ a smooth Victoreen-like function with absolute values normalized to the absorption jump of each spectrum. The experimental $k\chi(k)$ functions at 77, 300, and 410 K are shown in Fig. 1.

The moduli of Fourier transforms of the $k\chi(k)$ signals are shown in Fig. 2 for selected temperatures. The bimodal shape of the first-shell contribution, extending from 1.2 to 3.5 Å, is due to the resonant behavior of the complex backscattering amplitude of silver. The contribution of the first shell (four silver atoms at 2.82 Å) was singled out by Fourier back transform: The dotted lines in Fig. 2 represent asymmetric Hanning windows specifically tailored to the peak shapes.

The phases $\Phi(k)$ and amplitudes $A(k)$ were separately

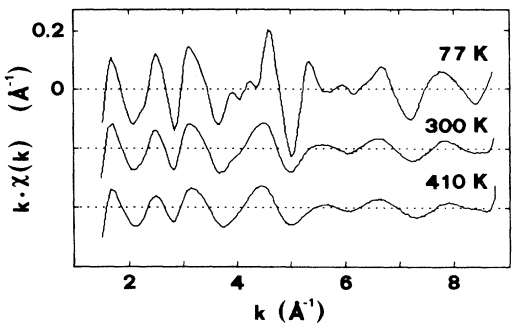

FIG. 1. EXAFS oscillations $k\chi(k)$ at the L_3 edge of iodine in β-AgI at 77, 300, and 410 K.

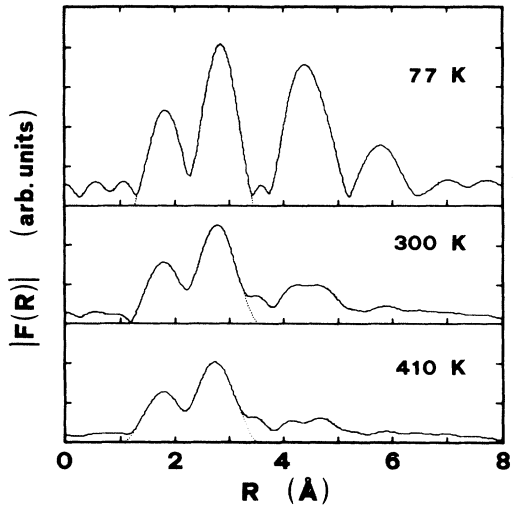

FIG. 2. Fourier transforms of the I L_3 EXAFS in β-AgI at 77, 300, and 410 K. The $k\chi(k)$ signal was limited to the k range 2.3–8 Å^{-1} by a square window. The dotted lines represent the first-shell back-transform window.

analyzed taking the 77 K signal as (harmonic) reference and truncating the cumulant expansion at the fourth-order term:

$$\Phi_s(k) - \Phi_r(k) = 2k\Delta C_1 - \frac{4}{3}k^3 C_3,$$
$$\ln \frac{A_s(k)}{A_r(k)} = -2k^2\Delta C_2 + \frac{2}{3}k^4 C_4, \tag{1}$$

where k is the photoelectron wave vector and s and r refer to signals at temperatures $T > 77$ K and $T = 77$ K, respectively (Fig. 3). The inflections at about 6 Å^{-1} reflect the resonant behavior of the backscattering amplitude of silver (relatively slight absolute uncertainties are amplified by the procedure of subtraction of phases). When

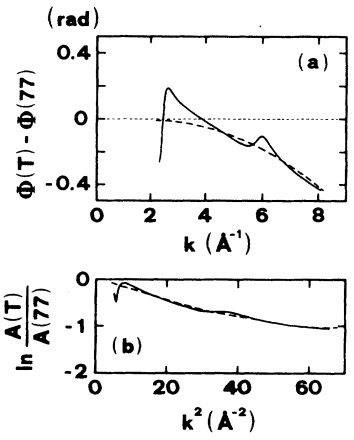

FIG. 3. Phase difference (a) and logarithm of amplitude ratio (b) of the first-shell EXAFS signals of AgI at 300 and 77 K (solid lines). The dashed lines are best fitting polynomials according to Eq. (1).

analyzing Ag K EXAFS (Ref. 10) smooth phase differences and amplitude ratios were obtained by subtracting the amplitude and phase shift from the experimental signal before the Fourier transform (Lee-Beni method;[23]) no significant differences were, however, found with the cumulants obtained through the standard procedure. In the present case, due to the shortness of the k range, the Lee-Beni procedure led to difficulties in the Fourier filtering procedure, and the standard procedure was considered more reliable. The anomalous behavior below 4 Å^{-1}, particularly evident in the phase difference as a crossing of the zero line, could not be modified by slight variations of the energy origin E_0. This behavior appeared to be mainly determined by the choice of the back-transform window (dotted lines in Fig. 2), limited to the main first-shell peak:[10] Neglecting broader features in the r space affects the low-k part of the EXAFS signal. Tests on EXAFS functions simulated from model distributions of distances have, however, shown that the enlargement of the back-transform window, while leading to apparently more reasonable behaviors of low-k phase differences, gives a larger discrepancy between the polynomial coefficients C_i obtained from EXAFS and actual cumulants of the original model distributions.[10] On the grounds of these tests, we chose to maintain the narrow back-transform window and consider only the range $k >$ 4 Å^{-1} in the procedure of fitting phases and amplitudes by Eq. (1) to obtain the polynomial coefficients C_i (Fig. 3). Neglecting the low-k signal also minimizes the possible error in phase analysis due to an inexact evaluation of the absolute energy origin E_0.[6,10] The reliability of this choice is *a posteriori* confirmed by the comparison with the results from Ag K-edge EXAFS (see below). The derivation of Eqs. (1), the underlying approximations, and the justification for assuming the 77 K reference as harmonic have been extensively discussed in Ref. 10.

The shortness of the effective k range of I L_3 EXAFS raises the question of the possible undetermination of the parameters. Our analysis gets four cumulants C_i, $i = 1,...,4$, from EXAFS; the separate analysis of phases and amplitudes avoids the correlation between the pairs of even and odd cumulants. For I L_3 EXAFS, taking into account that the phase analysis has been done for $k > 4$ Å^{-1}, the most conservative estimate of the number of relevant independent data points[1,24] is $N_i = 2\ \Delta k\ \Delta r/\pi \simeq 6$.

The cumulants obtained from the present analysis of I L_3 EXAFS are shown in Fig. 4 as diamonds and listed in Table I. The error bars have been determined by using different windows and k weighting in the Fourier filtering procedure and by allowing a relative shift of the energy origin ΔE_0 within $\pm$ 0.5 eV. To obtain absolute values of the second cumulant C_2 we utilized the standard procedure of fitting the slope of experimental points by an Einstein model and then upward shifting the experimental points to match the theoretical curve. This procedure is somewhat arbitrary, in view of the expected anharmonicity effects on C_2; it gives, however, the best estimate of C_2 at this stage of analysis. Its merit will be verified *a posteriori*, after anharmonic contributions have been evaluated. The Einstein frequency obtained

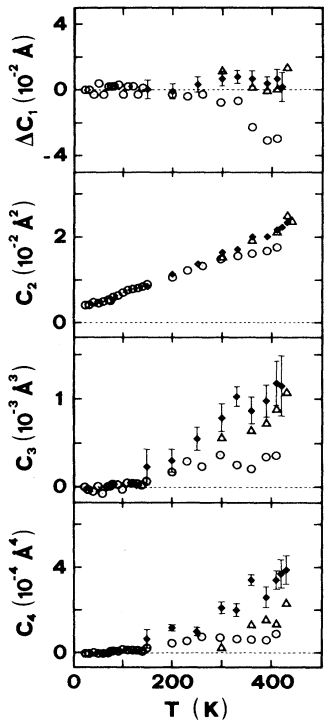

FIG. 4. Cumulants of the *effective* distributions of first-shell I-Ag distances in AgI: from analysis of I L_3 EXAFS (diamonds, present work); from analysis of Ag K EXAFS within the k range 2.5–16.5 Å^{-1} (circles, Ref. 10); from analysis of Ag K EXAFS limited to k_{max} = 10 Å^{-1} (triangles).

from the present cumulant analysis (2.61 THz) is slightly lower than the one obtained from the previous harmonic analysis of I L_3 EXAFS (2.65 THz).[22] This is not surprising, since harmonic analysis underestimates the MSRD's when anharmonic effects are present.

The previous cumulant analysis of Ag K EXAFS (Ref. 10) was done in the whole available k range 2.5–16.5 Å^{-1} at all temperatures; the resulting cumulants are shown as circles in Fig. 4. The regular temperature dependence of cumulants is broken above 300 K. A reduction of the k interval in fitting the phase differences and amplitude ratios did not appreciably modify this anomalous behavior. A satisfactory agreement with I L_3 results has now been obtained also above 300 K by reducing to k_{max}=10 Å^{-1} the analyzed range of Ag K EXAFS already from the Fourier transform window (triangles in Fig. 4). This suggests that the reduction with temperature of the convergence interval of the cumulant series has to be taken into account in EXAFS analysis already at the Fourier transform stage. The diamonds and triangles in Fig. 4 have been obtained from different samples, synchrotron radiation facilities, absorption edges, and data reduction procedures. Their differences, together with the error bars, allow us to estimate the overall uncertainty of cumulants.

III. RESULTS AND DISCUSSION

The polyomial coefficients C_i obtained from Eqs. (1) and shown as diamonds in Fig. 4 exhibit a regular temperature dependence; in particular C_3 and C_4 can be reasonably fitted by T^2 and T^3 curves, respectively. We assume, as a working hypothesis to be confirmed *a posteriori*, that within the I L_3 EXAFS range ($k < 8$ Å^{-1}) the cumulant series of the distribution of I-Ag distances is convergent and only the first four cumulants are significative. As a consequence, the EXAFS polynomial coefficients C_i are good estimates of the cumulants of the *effective* distribution of distances $P(r) = \rho(r)\exp(-2r/\lambda)/r^2$, where $\rho(r)$ is the *real* distribution and λ the photoelectron mean free path.[5]

A. Distribution of distances

Once the leading cumulants are known, the EXAFS signal can be extrapolated to $k = 0$ and Fourier transformed to obtain the *effective* distribution of distances $P(r,\lambda)$.[9] In Fig. 5 the *real* distributions of Ag-I distances reconstructed from cumulants at 300 and 370 are shown as solid lines. A k-independent mean free path λ=7 Å was considered; no significative variations were found by varying λ from 4 to 10 Å. The $\chi(k)$ function was built within the k intervals −8 to 8 and −10 to 10 Å^{-1} from the I L_3 and Ag K cumulants, respectively; no relevant differences were found in the distributions. The dashed

TABLE I. Cumulants of the effective distributions of I-Ag distances from the analysis of I L_3 EXAFS. The 77 K data have been used as a harmonic reference. Absolute values of the MSRD C_2 have been obtained by fitting an Einstein model to the slope of experimental ΔC_2 data.

T (K)	ΔC_1 (10^{-3} Å)		C_2 (10^{-2} Å^2)		C_3 (10^{-3} Å^3)		C_4 (10^{-4} Å^4)	
77	0.0		0.47		0.0		0.0	
150	-0.7	± 5.7	0.83	± 0.05	0.2	± 0.2	0.7	± 0.4
200	-1.1	± 4.7	1.12	± 0.03	0.3	± 0.1	1.2	± 0.1
250	3.1	± 4.6	1.36	± 0.04	0.55	± 0.13	1.0	± 0.2
300	6.7	± 4.4	1.63	± 0.01	0.79	± 0.15	2.1	± 0.3
330	7.8	± 3.8	1.71	± 0.01	1.03	± 0.11	2.0	± 0.3
360	6.7	± 4.6	2.00	± 0.01	0.87	± 0.15	3.4	± 0.2
390	3.7	± 4.1	2.00	± 0.03	0.98	± 0.16	2.6	± 0.5
410	6.5	± 5.7	2.17	± 0.05	1.18	± 0.25	3.4	± 0.4
420	1.5	± 8.9	2.23	± 0.05	1.15	± 0.34	3.7	± 0.6

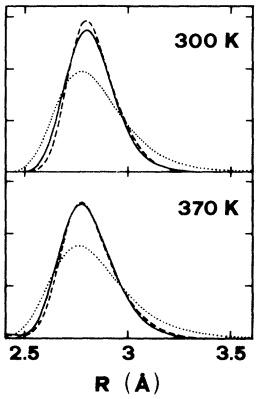

FIG. 5. *Real* distributions of I-Ag interatomic distances reconstructed from EXAFS cumulants at 300 and 370 K (solid lines). Also shown are the distributions of the excluded-volume model (dashed lines, Ref. 20) and the distributions calculated through molecular dynamics simulations (dotted lines, Ref. 26).

lines in Fig. 5 are the distributions of the excluded-volume model with parameters optimized by Hayes *et al.*[20] through a real-space analysis of Ag K EXAFS of AgI, Fourier transformed within the k range from 3.1 to 11 Å^{-1}. The agreement between the EXAFS-based distributions confirms that the working hypothesis on the convergence of the cumulant series is valid and that the cumulant method can be confidently utilized to get the distributions of distances in a model-independent way.

The superiority of the splice method with respect to the cumulant method for largely disordered systems has been recently demonstrated by tests on exponentially skewed distributions.[25] In the present case of AgI, the cumulant method without splicing is correctly working within the considered k range. In Ref. 10 it was shown that distributions of apparently similar shape, such as the excluded-volume and the exponentially skewed ones, can be characterized by very different convergence properties of the cumulant series.

The dotted lines in Fig. 5 have been obtained from molecular dynamics (MD) simulations[26] utilizing the pair potentials optimized by Parrinello *et al.* to reproduce the β to α phase transition in AgI.[27] The discrepancy between EXAFS and MD distributions is similar to that found in α phase[28] and can be attributed to the inadequacy of the interaction potential utilized in MD simulations to fully reproduce the correlation of vibrational motion of silver and iodine ions.[21,26]

The procedure outlined above allows the reconstruction of the *real* distribution of distances once the cumulants of the *effective* distribution and the photoelectron mean free path are known. We will now investigate the connection between the cumulants $\sigma^{(i)}$ of the *real* distribution and the cumulants C_i of the *effective* distribution. It is commonly assumed in the literature that the differences between the cumulants of order higher than 1 of the two distributions are negligible. This assumption relies on the similarity between the moments of the two distributions[5] or on calculations based on series expansion approximations.[8] The only non-negligible difference is considered to be the one between the first-order cumulants (average interatomic distances), for which[5,15,8]

$$C_1 - \sigma^{(1)} = -\frac{2\,\sigma^{(2)}}{\sigma^{(1)}}\left(1 + \frac{\sigma^{(1)}}{\lambda}\right). \qquad (2)$$

A difference smaller by a factor of 2 was recently suggested by Ishii on the basis of an independent calculation.[29]

To check the validity of these assumptions, we made a direct numerical computation of the first four cumulants on several model distributions with position, shape, and width comparable with those of AgI at and above room temperature: an exponentially skewed distribution $B\exp[-B(r - R_0)]$, with $B = 10, 15, 20$ Å^{-1},[6] and excluded-volume model for $T = 300, 370$ K.[20] The results are summarized in Table II as percent differences between the *effective* cumulants C_i and the *real* ones $\sigma^{(i)}$. The relative differences grow with growing cumulant order from about 5–8 % for C_2 to about 15–20 % for C_4, the cumulants of the effective distributions being generally lower than those of the real ones. As for the first-order cumulants, a good agreement is found with Eq. (2) (last column in Table II).

These conclusions show that the differences between cumulants of the real and effective distributions are not *a priori* negligible and increase with the extent of disorder. A direct check on the distributions reconstructed from

TABLE II. Percent differences between the first four cumulants of *effective* and *real* model distributions, C_i and $\sigma^{(i)}$, respectively. Three exponentially skewed $B\exp[-B(r - R_0)]$ and two excluded-volume (EV) distributions centered at R_0=2.82 Å have been considered, with different parameters B and temperatures T, respectively, and a photoelectron mean free path $\lambda = 7$ Å. The last column reports the percent discrepancy between the values of $C_1 - \sigma^{(1)}$ calculated in two ways: (a) by obtaining both C_1 and $\sigma^{(1)}$ from the corresponding distributions, (b) by obtaining C_1 from the cumulants $\sigma^{(1)}$ and $\sigma^{(2)}$ of the real distribution through Eq. (2).

Distribution	$i = 1$	$i = 2$	$i = 3$	$i = 4$	$\delta[C_1 - \sigma^{(1)}]$
Skewed B=20	-0.25	-2.9	-12.8	-16.5	3
Skewed B=15	-0.3	-5.4	-16	-21	3
Skewed B=10	-0.4	-10	-23	-28.9	8
EV $T = 300$	-0.4	-5	-5.6	+20	3
EV $T = 370$	-0.6	-7.6	-9	+11	4

the EXAFS of AgI was not possible at this stage because of the errors in computing cumulants due to the side lobes introduced by the Fourier transform procedure. A more accurate, although less direct, check will be made below.

B. EXAFS pair potential

In a classical approximation, say, above the Debye temperature (which for AgI is about 150 K), the real distribution of interatomic distances may be expressed as a canonical average:

$$\rho(r) = \frac{\int e^{-\beta V(r,\mathbf{r}^*)}\, d\mathbf{r}^*}{\int e^{-\beta V(r,\mathbf{r}^*)}\, dr\, d\mathbf{r}^*} = \frac{e^{-\beta V_E(r)}}{\int e^{-\beta V_E(r)}\, dr}, \quad (3)$$

where r is the distance between absorber and backscatterer atoms and $\mathbf{r}^*$ indicates the remaining $3N-1$ coordinates necessary to describe the positions of the N atoms of the crystal. A similar relation holds also for the effective distribution of distances $P(r,\lambda)$. The pair potential $V_E(r)$ depends on the statistically averaged behavior of all the atoms in the crystal and can in principle exhibit temperature dependence.[13]

By inverting Eq. (3), the pair potentials V_E have been calculated at different temperatures for both the effective and real distributions of I-Ag distances reconstructed from EXAFS cumulants. The resulting curves are shown in Figs. 6(a) and 6(b). The shape of the potential V_E is, to a large extent, temperature independent. The variation of the shape of the distance distributions $\rho(r)$ with temperature can then be accounted for by thermal disorder under an anharmonic potential. The equilibrium distance (minimum of the potential V_E) shifts towards lower values when increasing the temperature. This shift is larger for the effective than for the real distributions [triangles in Figs. 7(a) and 7(b), respectively]. A similar shift of the equilibrium position affects also the pair potentials obtained through Eq. (3) from the MD distributions [Fig. 6(c)]. This means that the shift reflects the peculiar properties of the interaction potentials in AgI, and cannot be attributed to artifacts in the EXAFS data reduction procedure.

The second- and higher-order cumulants only depend on the shape of the pair potential. Their temperature dependence should then exhibit the behavior expected for temperature-independent anharmonic pair potentials. The temperature dependence of the first cumulant, say, the average interatomic distance, reflects instead two joint effects: the anharmonicity of the pair potential and the shift of its equilibrium position.

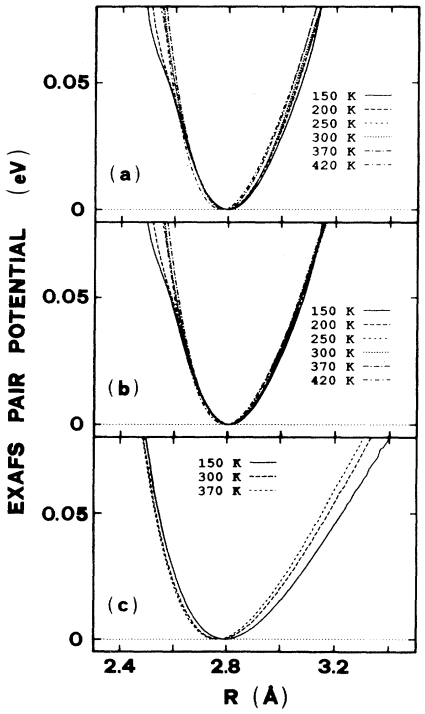

FIG. 6. EXAFS pair potentials of the *effective* (a) and *real* (b) distributions of I-Ag distances from EXAFS cumulants at various temperatures. Panel (c) shows the pair potentials of the distributions calculated through molecular dynamics simulations.

C. Temperature dependence of cumulants

The cumulants C_i of a distribution can be expanded (always in classical approximation) as a power series of temperature:[30]

$$\delta C_1 = -\sigma_0^2\, \gamma_3/2 + \cdots, \quad (4a)$$

$$C_2 = \sigma_0^2 + \sigma_0^4\, (\gamma_3^2 - \gamma_4/2) + \cdots, \quad (4b)$$

$$C_3 = -\sigma_0^4 \gamma_3 + \cdots, \quad (4c)$$

$$C_4 = \sigma_0^6\, (3\gamma_3^2 - \gamma_4) + \cdots . \quad (4d)$$

σ_0^2 and the γ_n are directly connected to the force constants of the pair potential V_E:

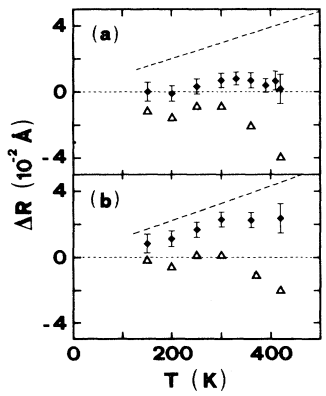

FIG. 7. Temperature dependence of average I-Ag interatomic distances for the *effective* (a) and *real* (b) distributions. The triangles represent the shifts of the equilibrium positions of the EXAFS pair potentials. The dashed lines correspond to the expansion due to potential anharmonicity. The diamonds are the values ΔC_1 obtained from EXAFS in panel (a), and the values $\Delta\sigma^{(1)}$, calculated through Eq. (2), in panel (b).

$$\gamma_n = \frac{\partial^n V(u)}{\partial u^n} \Big/ \frac{\partial^2 V(u)}{\partial u^2}, \quad \sigma_0^2 = K_B T \Big/ \frac{\partial^2 V(u)}{\partial u^2}, \tag{5}$$

where u is the deviation from equilibrium and partial derivatives are calculated for $u = 0$. δC_1 in Eq. (4a) is the variation in C_1 due to the potential anharmonicity; it does not include the contribution of the potential shift observed in the present case of AgI.

For a harmonic potential, $\gamma_n = 0$ for $n > 2$, C_2 linearly depends on temperature, and C_3 and C_4 are zero. The effect of anharmonicity is, to first order, the presence of an additional term proportional to T^2 in the expression of C_2 and the proportionality of C_3 and C_4 to second and third powers of T, respectively. Higher-order terms in Eqs. (4) can be non-negligible for strongly anharmonic potentials and/or for high temperatures.

From the pair potentials of Figs. 6(a) and 6(b) we calculated the force constants and the temperature dependence of cumulants through Eqs. (4). The results of this procedure are shown in Fig. 8 for the second, third, and fourth cumulants (the first cumulant will be considered below). The discrepancy between cumulants of effective and real distributions (solid and dashed lines, respectively) is consistent with the results of our previous analysis on model distributions (Table II). The diamonds in Fig. 8 are the original experimental cumulants C_i of the effective distribution.

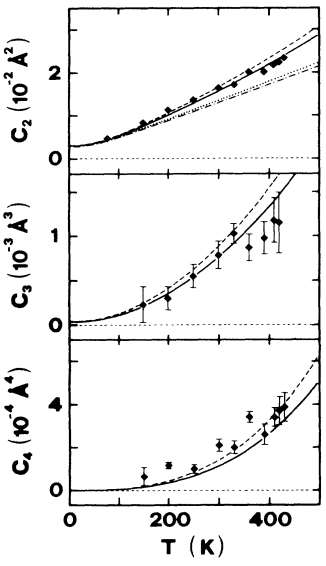

FIG. 8. Temperature dependence of second, third, and fourth cumulants. The diamonds represent the cumulants C_i of the *effective* distributions obtained from EXAFS as in Fig. 4. The lines have been calculated from the force constants of the EXAFS potential through Eqs. (4): Solid lines refer to *effective* distributions, dashed lines to *real* distributions. For the second cumulant (MSRD) also the first-order harmonic contribution is shown, represented by the Einstein model corresponding to the classical behavior at high temperatures (dash-dotted line for the *effective* distributions, dotted line for the *real* distributions).

The harmonic and first-order anharmonic contributions to the second cumulant (proportional to T and T^2, respectively) have been singled out. The linear harmonic contribution of the classical approximation has been replaced in Fig. 8 by the corresponding Einstein model (dash-dotted and dotted lines for effective and real distributions, respectively). The anharmonic contribution is not negligible: It amounts to about 20% of the total MSRD at 300 K, and is comparable with the anharmonic contribution estimated for CuBr by Tranquada and Ingalls.[15] A satisfactory agreement is found between the curve calculated for the effective distribution and the original experimental cumulants C_2 (solid line and diamonds in Fig. 8, respectively). This suggests that the use of a harmonic model to estimate the absolute values C_2 during data analysis did not produce appreciable errors. The Einstein frequency 2.61 THz best fitting the slope of experimental points has, however, little physical meaning, in view of the non-negligible anharmonic contribution. The right Einstein frequency to be used when comparing EXAFS results with harmonic force-constant models should be derived from the harmonic contribution to the second cumulant of the real distribution (dotted line in Fig. 8); in the present case it amounts to 2.9 THz.

As for the third and fourth cumulants, their temperature dependence is reasonably well reproduced by the first-order terms of Eqs. (4).

D. Thermal expansion and vibrational dynamics

Let us now consider the temperature dependence of the I-Ag distance. In Fig. 7 the triangles represent the shifts of the EXAFS pair potentials V_E of both (a) effective and (b) real distributions. The dashed lines represent the variations δC_1 of the interatomic distance induced by the anharmonicity of V_E and calculated through Eq. (4a). The diamonds are the experimental values ΔC_1 of the effective distributions in Fig. 7(a), and the corresponding values $\Delta\sigma^{(1)}$ of the real distributions calculated through Eq. (2) in Fig. 7(b). For both distributions the diamonds correspond, with good approximation, to the sum of the potential shift (triangles) and the expansion due to anharmonicity (dashed lines). This indirectly confirms the validity of Eq. (2) for our experimental data.

The thermal variation of interatomic distance in several compounds has recently been estimated from EXAFS through the ratio $C_3/2C_2$.[11,12] This procedure is not applicable in the case of AgI. The ratio $C_3/2C_2$ is equal (to a first approximation) to δC_1 of Eq. (4a); it then does not take into account the observed potential shift, which significantly contributes to the interatomic distance monitored by EXAFS in AgI. It would be interesting to check whether this temperature dependence of the EXAFS pair potential is present or relevant only in AgI or is shared also by other systems.

A further discussion concerns the difference between EXAFS results and crystallographic thermal expansion. The diamonds in Fig. 7(b), representing the variations of the mean values of the I-Ag distance distributions, exhibit a progressive growth with temperature of the order

of 0.01 Å over 200 K. The thermal expansion coefficient of AgI is, however, negative below 300 K: The corresponding variation in Ag-I distance between 100 and 300 K is negligible within $\pm 5 \times 10^{-4}$ Å.[19] Recently Yoshiasa *et al.* made single-crystal x-ray-diffraction (XRD) measurements on AgI between 123 and 413 K;[18] the resulting Ag-I distance, averaged over the three basal and one apical distances within the nearest-neighbors tetrahedron, is constant in temperature to within 0.002 Å.

The observed discrepancy between EXAFS and diffraction can be explained as follows. While diffraction measures the distance between the centers of the thermal ellipsoids, EXAFS measures a canonical average of instantaeous distances; the two values may differ substantially.[14] Let R be the distance between the centers of the thermal ellipsoids. The instantaneous interatomic distance r can be expanded in a power series of the thermal displacements $\vec{u}_0$ and $\vec{u}$ of the absorber and backscatterer atoms:[7,31]

$$r = R + \Delta u_{\parallel} + \frac{(\Delta u_{\perp})^2}{2R} + \cdots , \tag{6}$$

where $\Delta u_{\parallel} = \hat{R} \cdot (\vec{u}_j - \vec{u}_0)$ is the *radial* component of the relative atomic instantaneous displacement and $\Delta u_{\perp}$ is the corresponding *transverse* component. The canonical average $\langle \Delta u_{\parallel} \rangle$ is zero and $\langle r \rangle$ differs from R, to leading order, by $\langle (\Delta u_{\perp})^2 \rangle / 2R$.

The canonical average $\langle (\Delta u_{\parallel})^2 \rangle$ is the MSRD of the distribution of distances.[7] Like $\langle (\Delta u_{\parallel})^2 \rangle$, also $\langle (\Delta u_{\perp})^2 \rangle$ is sensitive to the correlation of motion of absorber and backscatterer atoms. The correlation function can, however, be different in radial and transverse directions.[32] An accurate evaluation of $\langle (\Delta u_{\parallel})^2 \rangle$ and $\langle (\Delta u_{\perp})^2 \rangle$ in a harmonic approximation would require full knowledge of the eigenfrequencies and eigenvectors of the dynamical matrix over all the Brillouin zone (BZ).[7,21] An order-of-magnitude evaluation has been attempted for AgI utilizing the eigenvectors calculated at the center of BZ by Cazzanelli *et al.*:[33] The value $\langle (\Delta u_{\parallel})^2 \rangle$ is in satisfactory agreement with the MSRD determined from EXAFS; $\langle (\Delta u_{\perp})^2 \rangle$ is about 10 times larger than $\langle (\Delta u_{\parallel})^2 \rangle$, its value being consistent with the apparent increase of Ag-I distances observed by EXAFS with respect to diffraction.

The most relevant contributions are given by the low-frequency optical modes, which distort the first-shell tetrahedral cage, driving the three basal atoms in phase and the apical atom out of phase with respect to the central atom. The out-of-phase motion, normal to the I-Ag bond direction, is responsible not only for the apparent increase of interatomic distance, but also for the very different temperature dependences observed for the MSRD of the first- and second-shell distances,[21] since it strongly affects the I-I MSRD but is substantially ininfluent on the I-Ag MSRD. Otherwise stated, the relatively large distortion of the tetrahedral cage induced by low-frequency optical modes does not contribute to the width of the distribution of I-Ag distances measured by EXAFS, Fig. 5. The distribution is then compatible not only with a liquidlike excluded-volume model,[20] which can explain the strong I-Ag correlation only in terms of long-wavelength acoustic phonons, but also with more complex dynamical models.

IV. CONCLUSIONS

In this work we have studied the effects of anharmonicity on the distribution of first-shell distances in AgI. To this aim, a cumulant analysis of temperature-dependent EXAFS at the L_3 edge of iodine in β-AgI has been done. Some results of a previous analysis made at the Ag K edge[10] have been confirmed with enhanced accuracy and results have been obtained concerning the physical significance of EXAFS cumulants for anharmonic systems.

The distributions of I-Ag interatomic distances and the corresponding pair potentials have been obtained up to the phase-transition temperature (420 K) directly from experimental EXAFS spectra. The only additional assumption was the fast convergence of the cumulant series within the considered EXAFS range; the validity of this assumption was justified by the regular temperature dependence of cumulants.

The anharmonic shape of the EXAFS pair potential is largely temperature independent while its equilibrium position shifts to lower values when the temperature is increased. The thermal variation of the interatomic distance measured by EXAFS depends on the superposition of these two contrasting effects: increase due to anharmonicity and decrease due to potential shift. The ratio $C_3/2C_2$, which depends only on the potential shape, is not adequate to account for thermal expansion in AgI. This suggests that further work should be done to clarify the relationship between the crystal potential and EXAFS pair potential.

A non-negligible difference has been found between the thermal variation of I-Ag distances measured by EXAFS and diffraction. Such a difference is in principle expected as a consequence of atomic vibrations normal to the bond direction. In the case of AgI the effect can be attributed to low-frequency optical modes which are responsible also for the peculiar difference of first- and second-shell MSRD's. The strong correlation of motion of iodine and silver nearest-neighbor ions is consistent not only with an excluded-volume model, but also with more realistic vibrational models featuring a strong distortion of the tetrahedral first-shell cage.

The harmonic and anharmonic contributions to the MSRD have been singled out on the basis of experimental data. This procedure will allow a more accurate comparison between EXAFS results and MSRD calculated through harmonic vibrational models.

The temperature dependences of the third and fourth cumulants have been shown to follow T^2 and T^3 first-order behaviors, respectively. This result gives the order of magnitude of anharmonicity and can be considered a check of the self-consistency of the procedure of data analysis.

The results of the present work, besides enlightening some peculiarities of AgI, suggest that a careful utilization of the cumulant analysis of EXAFS could give accurate structural and dynamical information on other systems affected by kinds and degrees of disorder similar to that of AgI.

ACKNOWLEDGMENTS

We would like to thank E. Burattini and the staff of Frascati Synchrotron Radiation Laboratories for technical support during the EXAFS measurements. We would also like to thank S. Cozzini and M. Ronchetti for their collaboration in the molecular dynamics calculations.

---

[1]P.A. Lee, P.H. Citrin, P. Eisenberger, and B.M. Kincaid, Rev. Mod Phys. **53**, 769 (1981).
[2]P. Eisenberger and G.S. Brown, Solid State Commun. **29**, 481 (1979).
[3]E.D. Crozier and A. Seary, Can. J. Phys. **58**, 1388 (1980).
[4]G. Dalba, D. Diop, P. Fornasini, and F. Rocca, J. Phys. Condens. Matter **6**, 3599 (1994).
[5]G. Bunker, Nucl. Instrum. Methods **207**, 437 (1983).
[6]E.D. Crozier, J.J. Rehr, and R. Ingalls, in *X-Ray Absorption*, edited by D.C. Koningsberger and R. Prins (Wiley, New York, 1988).
[7]G. Beni and P.M. Platzman, Phys. Rev. B **14**, 1514 (1976).
[8]J. Freund, R. Ingalls, and E.D. Crozier, Phys. Rev. B **39**, 12 537 (1989).
[9]E.A. Stern, Y. Ma, O. Hanske-Petitpierre, and C. Bouldin, Phys. Rev. B **46**, 687 (1992).
[10]G. Dalba, P. Fornasini, and F. Rocca, Phys. Rev. B **47**, 8502 (1993).
[11]T. Yokoyama, T. Satsukawa, and T. Ohta, Jpn. J. Appl. Phys. **28**, 1905 (1989).
[12]L. Wenzel, D. Arvanitis, H. Rabus, T. Lederer, K. Baberschke, and G. Comelli, Phys. Rev. Lett. **64**, 1765 (1990); L. Tröger, T. Yokoyama, D. Arvanitis, T. Lederer, M. Tischer, and K. Baberschke, Phys. Rev. B **49**, 888 (1994).
[13]J. Munstre de Leon, S.D. Conradson, I. Batistić, A.R. Bishop, I.D. Raistrick, M.C. Aronson, and F.H. Garzon, Phys. Rev. B **45**, 2447 (1992).
[14]B.T.M. Willis and A.W. Pryor, *Thermal Vibration in Crystallography* (Cambridge University Press, Cambridge, England, 1975).
[15]J.M. Tranquada and R. Ingalls, Phys. Rev. B **28**, 3520 (1983).
[16]E.A. Stern, P. Livins, and Z. Zhang, Phys. Rev. B **43**, 8850 (1991).
[17]E. Sevillano, H. Meuth, and J.J. Rehr, Phys. Rev. B **20**, 4908 (1979).
[18]A. Yoshiasa, K. Koto, F. Kanamaru, S. Emura, and H. Horiuchi, Acta Crystallogr. B **43**, 434 (1987).
[19]Y.S. Touloukian, R.K. Kirby, R.E. Taylor, and P.D. Desai, *Thermophysical Properties of Matter* (Plenum, New York, 1977), Vol. 13.
[20]T.M. Hayes, J.B. Boyce, and J.L. Beeby, J. Phys. C **11**, 2931 (1978).
[21]G. Dalba, P. Fornasini, F. Rocca, and S. Mobilio, Phys. Rev. B **41**, 9668 (1990).
[22]G. Dalba, P. Fornasini, and F. Rocca, J. Phys. Condens. Matter **4**, 1121 (1992).
[23]P.A. Lee and G. Beni, Phys. Rev. B **15**, 2862 (1977).
[24]E.A. Stern, Phys. Rev. B **48**, 9825 (1993).
[25]I. Ono, T. Yokoyama, H. Sato, K. Kaneyuki, and T. Ohta, Jpn. J. Appl. Phys. **32**, Suppl. 32-2, 83 (1993).
[26]G. Dalba, P. Fornasini, R. Gotter, S. Cozzini, M. Ronchetti, and F. Rocca, Solid State Ion. **69**, 13 (1994).
[27]M. Parrinello, A. Rahman, and P. Vashishta, Phys. Rev. Lett. **50**, 1073 (1983).
[28]A. Rahman and P. Vashishta, in *The Physics of Superionic Conductors and Electrode Materials*, edited by J.W. Perram, Vol. 92 of *NATO Advanced Study Institute, Series B: Physics* (Plenum, New York, 1980).
[29]T. Ishii, J. Phys. Condens. Matter **4**, 8029 (1992).
[30]J. Tranquada, Ph.D. thesis, University of Washington, Seattle, 1983.
[31]W.R. Busing and H.R. Levy, Acta Crystallogr. **17**, 142 (1963).
[32]O.H. Nielsen and W. Weber, J. Phys. C **13**, 2449 (1980).
[33]E. Cazzanelli, A. Fontana, G. Mariotto, F. Rocca, V. Mazzacurati, G. Ruocco, and A. Signorelli, Phys. Rev. B **38**, 10 883 (1988).